



Research paper

Design and synthesis of novel bicalutamide and enzalutamide derivatives as antiproliferative agents for the treatment of prostate cancer



Marcella Bassetto¹, Salvatore Ferla^{*1}, Fabrizio Pertusati¹, Sahar Kandil, Andrew D. Westwell, Andrea Brancale, Christopher McGuigan

School of Pharmacy and Pharmaceutical Sciences, Redwood Building, King Edward VII Avenue, CF10 3NB, Cardiff, Wales, UK

ARTICLE INFO

Article history:

Received 30 November 2015

Received in revised form

20 April 2016

Accepted 21 April 2016

Available online 22 April 2016

This work is dedicated to the memory of Prof. Chris McGuigan, a great colleague and scientist, invaluable source of inspiration and love for research.

Keywords:

Bicalutamide

Enzalutamide

Prostate cancer

Perfluoroalkyl

Androgen receptor

Antiproliferative activity

ABSTRACT

Prostate cancer (PC) is one of the major causes of male death worldwide and the development of new and more potent anti-PC compounds is a constant requirement. Among the current treatments, (R)-bicalutamide and enzalutamide are non-steroidal androgen receptor antagonist drugs approved also in the case of castration-resistant forms. Both these drugs present a moderate antiproliferative activity and their use is limited due to the development of resistant mutants of their biological target.

Insertion of fluorinated and perfluorinated groups in biologically active compounds is a current trend in medicinal chemistry, applied to improve their efficacy and stability profiles. As a means to obtain such effects, different modifications with perfluoro groups were rationally designed on the bicalutamide and enzalutamide structures, leading to the synthesis of a series of new antiproliferative compounds. Several new analogues displayed improved *in vitro* activity towards four different prostate cancer cell lines, while maintaining full AR antagonism and therefore representing promising leads for further development.

Furthermore, a series of molecular modelling studies were performed on the AR antagonist conformation, providing useful insights on potential protein-ligand interactions.

© 2016 The Authors. Published by Elsevier Masson SAS. This is an open access article under the CC BY license (<http://creativecommons.org/licenses/by/4.0/>).

1. Introduction

Prostate cancer (PC) is a leading cause of male death worldwide and it is the most frequently diagnosed cancer among men aged 65–74 [1]. The prognosis varies greatly, being highly dependent on a number of factors such as stage of diagnosis, race and age. Currently, PC treatment includes androgen deprivation, surgery, radiation, endocrine therapy and radical prostatectomy.

PC cell growth is strongly dependent on androgens, therefore blocking their effect can be beneficial to the patient's health. Such outcomes can be achieved by antagonism of the androgen receptor (AR) using anti-androgen drugs, which have been extensively explored either alone or in combination with castration [2]. Flutamide (Eulexin[®]) (1) (in its active form as hydroxyflutamide (2)),

bicalutamide (Casodex[®]) (3), nilutamide (Niladron[®]) (4) and enzalutamide (previously called MDV3100) (Xtandi[®]) (5) are all non-steroidal androgen receptor antagonists approved for the treatment of PC (Fig. 1). In many cases, after extended treatment over several years, these anti-androgens become ineffective and the disease may progress to a more aggressive and lethal form, known as castration resistant prostate cancer (CRPC). The major cause of this progressive disease is the emergence of different mutations on the AR, which cause the anti-androgen compounds to function as agonists, making them tumour-stimulating agents [3].

Among the drugs used for the treatment of PC, bicalutamide and enzalutamide selectively block the action of androgens while presenting fewer side effects in comparison with other AR antagonists [4–6]. The structure of these molecules is characterised by the presence of a trifluoromethyl substituted anilide, which appears to be critical for biological activity (Fig. 1). As a means to improve the anti-proliferative activity of these compounds, and in order to exploit the well established potential of the fluorine atom in enhancing the pharmacological properties and drug-like

* Corresponding author.

E-mail address: Ferlas1@cardiff.ac.uk (S. Ferla).

¹ These authors contributed equally to this work.

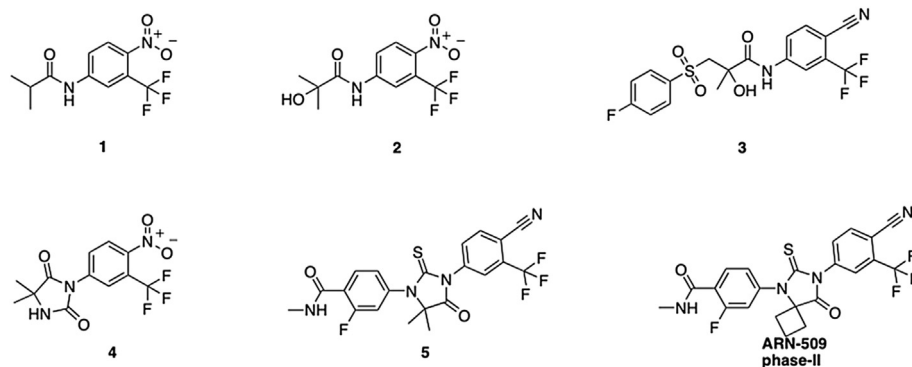


Fig. 1. Structure of anti-androgen small molecules approved by FDA or in clinical development for the treatment of PC.

physicochemical characteristics of candidate compounds [7–9], a wide array of diverse new structures has been rationally designed and synthesised, through the introduction of fluoro-, trifluoromethyl- and trifluoromethoxy groups in diverse positions of both aromatic rings of the parent scaffolds. Our modifications resulted in a marked improvement of *in vitro* anti-proliferative activities on a range of human PC cell lines (VCap, LNCaP, DU-145 and 22RV1). In addition, we probed full versus partial AR antagonism for our new compounds.

2. Results and discussion

Trifluoromethyl and trifluoromethoxy functions were systematically inserted on both aromatic rings of bicalutamide and enzalutamide, with the aim to explore the effect of perfluoro groups on their biological activity. As a means to further expand structure-activity relationship studies, the insertion of different linkers was also envisaged, along with the replacement of the bicalutamide methyl group with a trifluoromethyl function.

The main proposed modifications are summarised in Fig. 2.

2.1. Chemistry

Several reported methods for the synthesis of racemic bicalutamide were explored to find a rapid methodology that would allow the preparation of a wide range of new derivatives [10–12]. Modification and optimization of these procedures led to the development of the synthetic pathway shown in Scheme 1. Phenylacrylamides **12–16** were prepared by reacting the corresponding aniline (**7–11**) with methacryloyl chloride (**6**) in dimethylacetamide (DMA), modifying a reported methodology [10]. In particular, due to the presence of electron withdrawing

groups (nitro, cyano, trifluoromethyl) in different positions, anilines **7–11** were in some cases (**9** and **10** in particular) of low reactivity towards nucleophilic displacement. Synthetic efforts were made to achieve good yields (Supplementary data). Phenylacrylamides **12–16** were converted into the corresponding epoxides **17–21** in the presence of a large excess of hydrogen peroxide and trifluoroacetic anhydride in dichloromethane [11]. Opening of the epoxide rings of **17–21** with commercially available phenols and thiophenols gave a series of ethers (**27–31**) and thioether derivatives (**22–26**), respectively, in good yields after purification by column chromatography [11]. Thioethers **22–25** were finally oxidised to the corresponding sulfones **32–35** using mCPBA, maintaining the temperature at 25 °C [12]. Racemic bicalutamide (**3**) was prepared as a positive control following this route.

Since *R*-bicalutamide is known to be the most active enantiomer [13], chiral synthesis of selected *R*-bicalutamide analogues was carried out as shown in Scheme 2. (*R*)-*N*-Methacryloylproline **37**, prepared using (*R*)-proline (**36**) and methacryloyl chloride (**6**), was reacted with *N*-bromosuccinimide in DMF to afford bromolactone **38** as a single enantiomer [14]. Acid hydrolysis of **38** resulted in the formation of bromohydrin acid **39**, which was then converted into the corresponding chiral anilide (**40–41**) [14]. Amide derivatives **40–41** were reacted with the sodium salt of different commercial thiophenols in tetrahydrofuran to give, after purification by silica gel chromatography, the desired (*R*)-thioethers (**42–44**) [15]. Reaction of amide **40** with the sodium salt of 4-cyanophenol gave the reference compound (*S*)-enobosarm (**44e**). Oxidation of thioethers **42–43** with mCPBA provided sulfones **45–46**, with the desired *R* absolute configuration [12]. Reference (*R*)-bicalutamide (**45a**) was prepared following this synthetic route.

For one of the most active compounds initially found, **23d**, replacement of the central methyl group with an extra trifluoromethyl function was planned and carried out (Scheme 3).

3-Bromo-1,1,1-trifluoroacetone (**48**) was coupled with thiophenol **47** to afford **49**, which was then converted into cyano derivative **50** using potassium cyanide and 25% sulfuric acid [16]. Intermediate **51** was obtained after refluxing **50** in concentrated HCl and glacial acetic acid. Coupling of **51** with commercially available 4-nitro-3-(trifluoromethyl)aniline **8** yielded the desired amide **52**.

Several methods have been reported for the preparation of enzalutamide, all showing as a synthetic challenge the formation of the *N*-substituted thiohydantoin ring [17–19]. The method selected in this study was a three-step synthesis involving the preparation of different isothiocyanates (**54–58**), obtained in quantitative yield after treating the corresponding aniline (**7–10**, **53**) with thiophosgene (Scheme 4) [17]. Reaction conditions were optimised for the different anilines used, with **9** and **10** requiring higher

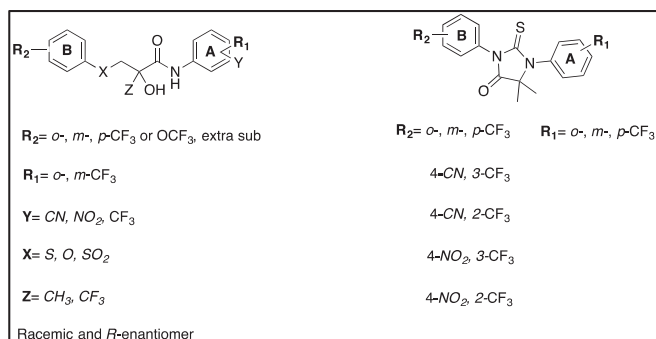
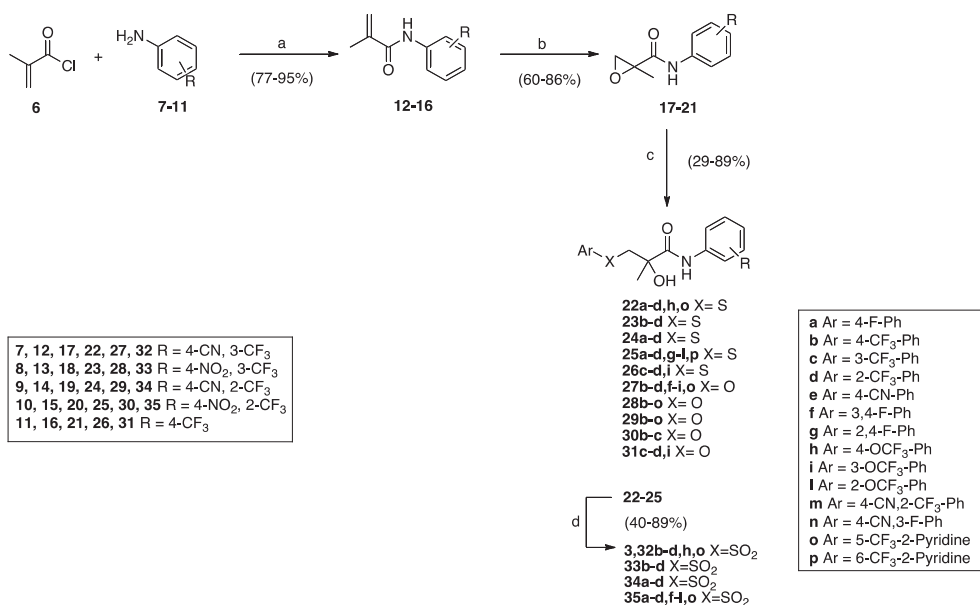
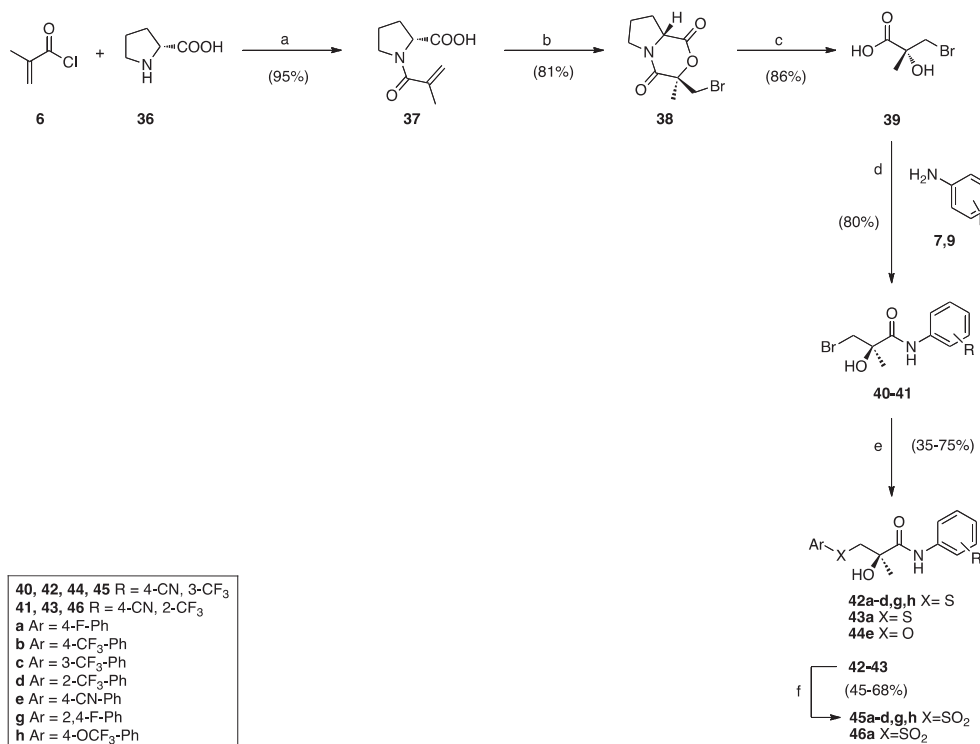


Fig. 2. Proposed modifications on bicalutamide and enzalutamide scaffolds.



Scheme 1. Synthetic pathway for the synthesis of racemic bicalutamide analogues adapted from reported procedures [10–12]. Reagents and conditions: (a) **6** (8 equiv.), DMA, RT, 3 h; (b) H₂O₂ (4 equiv.)/(CF₃CO)₂O (5 equiv.), DCM, RT, 24 h; (c) NaH (1.2 equiv.), **17–21** (1.2 equiv.), THF, RT, 24 h; (d) mCPBA (1.4 equiv.), DCM, RT, 4–6 h.

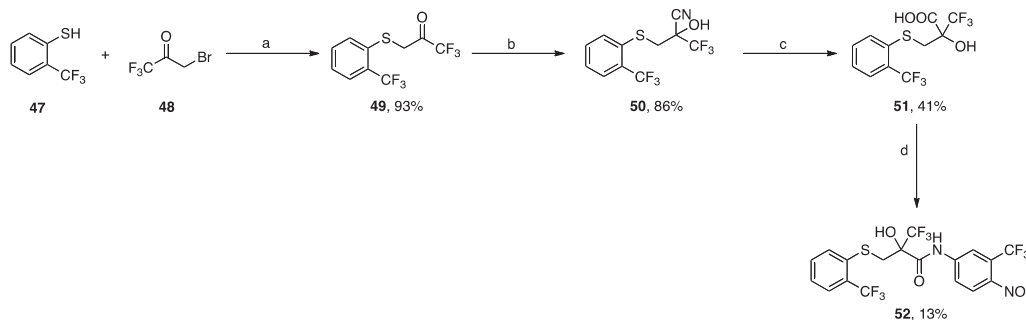


Scheme 2. Synthesis of (*R*)-bicalutamide derivatives [12,14,15]. Reagents and conditions: (a) **6** (1 equiv.), 2N NaOH, acetone, 0 °C to 10–11 °C, 3 h; (b) NBS, DMF, argon, 3 days, RT followed by H₂O, RT, 12–24 h; (c) 24% HBr, reflux, 1 h; (d) **39** (1 equiv.), SOCl₂ (1.2 equiv.), DMA, –10 °C, 2 h followed by **79** (1 equiv.), DMA, RT, o.n.; (e) **40/41** (1 equiv.), phenol/thiophenol (1.2 equiv.), 60% NaH (1.2 equiv.), THF, RT, 24 h; (f) mCPBA (1.4 equiv.), DCM, RT, 4–6 h.

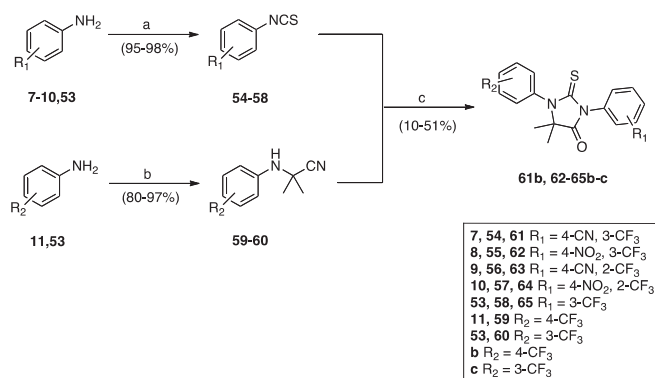
temperature, longer reaction time and the addition of extra equivalents of thiophosgene due to their low reactivity. Strecker reaction of substituted anilines (**11**, **53**) with acetone and trimethylsilyl cyanide generated the desired cyanomines **59–60**. Reaction of **59–60** with isothiocyanates **54–58** in DMF followed by the addition of HCl and MeOH gave the desired thiohydantoin **61–65**. The last reaction step was characterized by poor yields possibly due

to low reactivity and the formation of several side products (mainly due to the degradation of the reagents into the original starting anilines). Moreover, attempted preparation of enzalutamide derivatives **71b** and **71d**, in which the nitro and cyano groups are removed, was unsuccessful following this route.

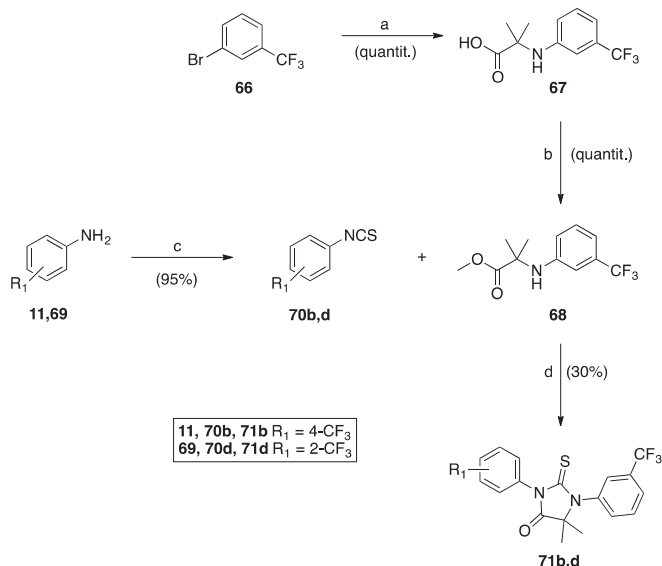
An alternative method reported for the preparation of enzalutamide was investigated to obtain **71b** and **71d** (Scheme 5) [19].



Scheme 3. Synthetic strategy used in the synthesis of **52**. Reagents and conditions: (a) NaH (1 equiv.), THF, 0 °C to RT, 3 h; (b) KCN (1.2 equiv.), 25% H₂SO₄, 0 °C to RT, 20 h; (c) HCl, AcOH, reflux, 24 h; (d) **8**, SOCl₂ (1.3 equiv.), DMA, RT, 72 h.



Scheme 4. Synthetic strategy toward enzalutamide derivatives. Adapted from reported procedure [17]. Reagents and conditions: (a) CCl₄ (1.5 equiv.), NaHCO₃, H₂O, DCM, RT, 24 h; (b) TMSCN (5.1 equiv.), acetone, 80 °C, 12 h; (c) DMF, RT 48 h, followed by HCl, MeOH, reflux, 6 h.



Scheme 5. Synthetic strategy toward enzalutamide derivatives **71b-d**. Adapted from a reported procedure [19]. Reagents and conditions: (a) 2-aminoisobutyric acid (1.5 equiv.), K₂CO₃ (6.5 equiv.), CuCl (0.2 equiv.), 2-acetylcyclohexanone (0.2 equiv.), DMF, H₂O, 105 °C, 14 h; (b) MeI (1.2 equiv.), K₂CO₃ (1.2 equiv.), H₂O, DMF, 40 °C, 1 h; (c) CCl₄ (1.5 equiv.), NaHCO₃, H₂O, DCM, RT, 24 h; (d) DMSO, IPAc, 84 °C, 14 h.

Commercially available 3-bromobenzotrifluoride (**66**) was coupled with 2-aminoisobutyric-acid to obtain amino propionic acid

derivative **67**, which was then converted into its methyl ester **68** after treatment with iodomethane. Reaction of **68** with different isothiocyanates (**70b, d**) yielded the desired thiohydantoin **71b** and **71d**. Following this procedure, standard enzalutamide (**5**) was also prepared.

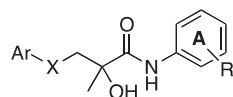
2.2. Antiproliferative assay

Antiproliferative activity of the newly synthesized compounds was initially evaluated with an *in vitro* 2D monolayer assay using four human prostate cancer cell lines (LNCaP, 22Rv1, VCaP, and DU145). LNCaP, VCaP and 22Rv1 exhibit some androgen sensitivity, whereas DU145 is hormone-insensitive. The assay allows determination of the compound's capacity to inhibit survival and/or cell proliferation. The antiproliferative results are reported in [Tables 1 and 2](#) (absolute IC₅₀ in μM).

The overall activity of the four reference compounds (**3, 5, 45a, 44e**) is consistent with previous reported data for some of these specific cell lines and it represents a confirmation of the reliability of the test [20–22]. 70% of our new derivatives performed better than bicalutamide, either as a racemic mixture or pure *R*-isomer (**3, 45a**), significantly improving its antiproliferative activity up to 50-fold (overall antiproliferative activity in the four cell lines reported as geometric mean).

Most inhibitors showed concentration-dependent activity against the four prostate cancer cell lines, with mean IC₅₀ values ranging from 1.6 μM to >100 μM. Active inhibitors showed sigmoidal concentration–effect curves with total cell kill at high concentrations (Supplementary data). Although the overall antiproliferative activity seems to be the result of the whole structure of each single derivative, a general SAR can be identified, considering three main structural components: linker X, aromatic ring A and aromatic ring B. Thioether or ether compounds (X = S or O) are associated with better antiproliferative activity than the corresponding sulfone derivatives (X = SO₂), with a decrease of effect in the sulfones up to eight fold (i.e. **251** and **281** vs **351**; **23d** & **28d** vs **33d**; **42d** vs **45d**; **22d** & **27d** vs **32d**; **23c** & **28c** vs **33c**). These data are consistent with previous work, in which thioether derivatives of SARMs (selective androgen receptor modulators) were found to be more active than the corresponding sulfones [20]. However, different newly prepared sulfones showed improved antiproliferative activity in comparison with the standard bicalutamide, with a decrease of IC₅₀ values up to two-fold (i.e. **33c, 33b, 45b**, etc.). Replacement of the sulfur atom with oxygen is in general associated with retained activity (i.e. **23c** vs **28c**; **22c** vs **27c**), with only few cases of decreased activity in comparison with the thioether analogues (i.e. **251** vs **281**; **23d** vs **28d**), probably due to the combined effect of the substituent on aromatic ring B and the linker. Several new ether derivatives performed better than the

Table 1
Antiproliferative activity for bicalutamide/enobosarm derivatives. All data are mean values from triplicate experiments.



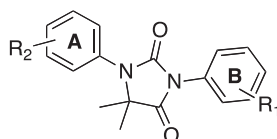
Compound	Ar (B ring)	X	R (A ring)	Absolute IC ₅₀ (μM)				
				22Rv1	DU-145	LNCAp	VCaP	Geo.mean
3 (Bic.)	4-F-Ph	SO ₂	4-CN, 3-CF ₃	49.58	49.20	45.27	68.37	52.42
44e (S-Eno)	4-CN-Ph	O	4-CN, 3-CF ₃	24.77	44.55	20.90	24.47	27.41
45a (R-Bic.)	4-F-Ph	SO ₂	4-CN, 3-CF ₃	46.25	45.41	45.20	51.61	47.05
22b	4-CF ₃ -Ph	S	4-CN, 3-CF ₃	NA				
22c	3-CF ₃ -Ph	S	4-CN, 3-CF ₃	5.56	10.58	5.03	9.23	7.23
22d	2-CF ₃ -Ph	S	4-CN, 3-CF ₃	5.06	7.73	4.91	7.51	6.16
22h	4-OCF ₃ -Ph	S	4-CN, 3-CF ₃	46.62	64.01	42.81	40.33	47.64
22o	4-CF ₃ -2-Pyridine	S	4-CN, 3-CF ₃	53.91	84.10	80.72	89.27	75.60
23b	4-CF ₃ -Ph	S	4-NO ₂ , 3-CF ₃	16.43	22.52	28.71	21.17	21.78
23c	3-CF ₃ -Ph	S	4-NO ₂ , 3-CF ₃	5.07	8.73	6.44	8.64	7.04
23d	2-CF ₃ -Ph	S	4-NO ₂ , 3-CF ₃	4.6	7.57	4.78	4.45	5.17
24a	4-F-Ph	S	4-CN, 2-CF ₃	30.08	43.28	26.45	45.48	35.37
24b	4-CF ₃ -Ph	S	4-CN, 2-CF ₃	NA				
24c	3-CF ₃ -Ph	S	4-CN, 2-CF ₃	15.16	21.05	11.26	23.48	17.04
24d	2-CF ₃ -Ph	S	4-CN, 2-CF ₃	11.64	18.42	10.72	18.27	14.32
25a	4-F-Ph	S	4-NO ₂ , 2-CF ₃	17.63	26.40	11.93	21.10	18.50
25b	4-CF ₃ -Ph	S	4-NO ₂ , 2-CF ₃	14.63	19.20	8.66	17.07	14.28
25c	3-CF ₃ -Ph	S	4-NO ₂ , 2-CF ₃	12.58	14.35	10.07	16.51	13.16
25d	2-CF ₃ -Ph	S	4-NO ₂ , 2-CF ₃	11.97	17.53	11.66	12.79	13.30
25f	3,4-F-Ph	S	4-NO ₂ , 2-CF ₃	83.59	100	83.04	100	91.28
25g	2,4-F-Ph	S	4-NO ₂ , 2-CF ₃	14.93	21.43	11.00	16.64	15.56
25h	4-OCF ₃ -Ph	S	4-NO ₂ , 2-CF ₃	61.92	69.59	100	100	81.02
25i	3-OCF ₃ -Ph	S	4-NO ₂ , 2-CF ₃	15.80	21.63	9.15	15.88	14.93
25l	2-OCF ₃ -Ph	S	4-NO ₂ , 2-CF ₃	4.64	6.57	3.31	5.27	4.80
25o	4-CF ₃ -2-Pyridine	S	4-NO ₂ , 2-CF ₃	13.58	19.74	11.06	17.18	15.02
25p	5-CF ₃ -2-Pyridine	S	4-NO ₂ , 2-CF ₃	11.52	14.03	5.52	17.36	11.15
26c	3-CF ₃ -Ph	S	4-CF ₃	18.57	30.71	22.56	19.50	22.44
26d	2-CF ₃ -Ph	S	4-CF ₃	5.20	8.76	7.22	5.86	6.63
26i	3-OCF ₃ -Ph	S	4-CF ₃	15.90	27.84	13.88	18.82	18.44
27b	4-CF ₃ -Ph	O	4-CN, 3-CF ₃	6.91	16.28	6.45	9.65	9.15
27c	3-CF ₃ -Ph	O	4-CN, 3-CF ₃	5.89	10.84	8.31	9.04	8.32
27d	2-CF ₃ -Ph	O	4-CN, 3-CF ₃	11.55	17.32	9.68	16.60	13.39
27f	3,4-F-Ph	O	4-CN, 3-CF ₃	35.54	45.19	18.98	25.64	29.73
27g	2,4-F-Ph	O	4-CN, 3-CF ₃	34.00	44.26	37.30	38.69	38.39
27h	4-OCF ₃ -Ph	O	4-CN, 3-CF ₃	17.20	18.36	13.56	17.59	16.57
27i	3-OCF ₃ -Ph	O	4-CN, 3-CF ₃	9.79	16.36	9.83	9.91	11.17
27o	4-CF ₃ -2-Pyridine	O	4-CN, 3-CF ₃	100	100	100	100	100
28b	4-CF ₃ -Ph	O	4-NO ₂ , 3-CF ₃	16.19	25.93	17.24	10.91	16.76
28c	3-CF ₃ -Ph	O	4-NO ₂ , 3-CF ₃	8.58	10.02	9.91	10.28	9.68
28d	2-CF ₃ -Ph	O	4-NO ₂ , 3-CF ₃	20.16	35.20	22.60	27.16	25.69
28e	4-CN-Ph	O	4-NO ₂ , 3-CF ₃	30.92	32.68	18.69	26.88	26.69
28f	3,4-F-Ph	O	4-NO ₂ , 3-CF ₃	18.54	21.61	14.50	18.92	18.21
28g	2,4-F-Ph	O	4-NO ₂ , 3-CF ₃	20.16	22.39	10.06	20.92	17.56
28h	4-OCF ₃ -Ph	O	4-NO ₂ , 3-CF ₃	7.53	10.43	17.66	19.55	12.83
28i	3-OCF ₃ -Ph	O	4-NO ₂ , 3-CF ₃	9.31	13.14	9.95	9.60	10.40
28l	2-OCF ₃ -Ph	O	4-NO ₂ , 3-CF ₃	6.60	9.88	7.04	9.61	8.15
28m	4-CN,2-CF ₃ -Ph	O	4-NO ₂ , 3-CF ₃	5.55	7.65	5.69	8.38	6.71
28n	4-CN,3-F-Ph	O	4-NO ₂ , 3-CF ₃	11.77	16.39	7.71	12.39	11.65
28o	4-CF ₃ -2-Pyridine	O	4-NO ₂ , 3-CF ₃	35.22	100	36.51	100	59.88
29b	4-CF ₃ -Ph	O	4-CN, 2-CF ₃	29.91	32.39	28.61	23.02	28.26
29c	3-CF ₃ -Ph	O	4-CN, 2-CF ₃	18.70	32.12	15.23	21.59	21.08
29d	2-CF ₃ -Ph	O	4-CN, 2-CF ₃	19.60	33.17	14.03	21.93	21.15
29e	4-CN-Ph	O	4-CN, 2-CF ₃	42.935	100	34.722	61.370	55.00
29f	3,4-F-Ph	O	4-CN, 2-CF ₃	37.03	41.93	34.80	47.18	39.95
29g	2,4-F-Ph	O	4-CN, 2-CF ₃	60.92	99.48	30.64	50.62	55.37
29h	4-OCF ₃ -Ph	O	4-CN, 2-CF ₃	27.99	34.64	27.65	22.37	27.83
29i	3-OCF ₃ -Ph	O	4-CN, 2-CF ₃	28.65	35.86	63.39	56.34	43.76
29l	2-OCF ₃ -Ph	O	4-CN, 2-CF ₃	16.68	27.09	33.83	43.85	28.61
29m	4-CN,2-CF ₃ -Ph	O	4-CN, 2-CF ₃	18.45	27.52	9.39	17.70	17.04
29n	4-CN,3-F-Ph	O	4-CN, 2-CF ₃	45.34	68.78	78.27	77.20	65.89
29o	4-CF ₃ -2-Pyridine	O	4-CN, 2-CF ₃	100	100	100	100	100
30b	4-CF ₃ -Ph	O	4-NO ₂ , 2-CF ₃	18.93	22.08	13.57	18.56	18.01
30c	3-CF ₃ -Ph	O	4-NO ₂ , 2-CF ₃	15.17	18.14	12.93	19.34	16.20
31c	3-CF ₃ -Ph	O	4-CF ₃	25.68	27.45	18.16	18.64	22.100
31d	2-CF ₃ -Ph	O	4-CF ₃	6.42	26.41	6.98	11.49	10.80
31i	3-OCF ₃ -Ph	O	4-CF ₃	15.43	29.40	2.16	4.28	8.05

Table 1 (continued)

Compound	Ar (B ring)	X	R (A ring)	Absolute IC ₅₀ (μM)				
				22Rv1	DU-145	LNCaP	VCaP	Geo.mean
32b	4-CF ₃ -Ph	SO ₂	4-CN, 3-CF ₃	21.54	32.84	20.05	29.11	25.345
32c	3-CF ₃ -Ph	SO ₂	4-CN, 3-CF ₃	20.954	39.112	14.94	39.66	26.40
32d	2-CF ₃ -Ph	SO ₂	4-CN, 3-CF ₃	46.55	55.03	42.74	58.55	50.32
32h	4-OCF ₃ -Ph	SO ₂	4-CN, 3-CF ₃	17.02	27.28	31.64	32.81	26.35
32o	4-CF ₃ -2-Pyridine	SO ₂	4-CN, 3-CF ₃	100	100	100	100	100
33b	4-CF ₃ -Ph	SO ₂	4-NO ₂ , 3-CF ₃	18.66	24.68	17.94	31.53	22.59
33c	3-CF ₃ -Ph	SO ₂	4-NO ₂ , 3-CF ₃	16.14	31.62	16.20	30.83	22.47
33d	2-CF ₃ -Ph	SO ₂	4-NO ₂ , 3-CF ₃	18.56	37.51	25.70	27.55	26.50
34a	4-F-Ph	SO ₂	4-CN, 2-CF ₃	77.00	100	91.59	65.22	82.36
34b	4-CF ₃ -Ph	SO ₂	4-CN, 2-CF ₃	27.87	44.56	32.93	43.29	36.48
34c	3-CF ₃ -Ph	SO ₂	4-CN, 2-CF ₃	34.35	45.94	32.08	44.92	38.83
34d	2-CF ₃ -Ph	SO ₂	4-CN, 2-CF ₃	98.82	100	74.02	100	92.48
35a	4-F-Ph	SO ₂	4-NO ₂ , 2-CF ₃	46.67	60.73	38.65	58.21	50.25
35b	4-CF ₃ -Ph	SO ₂	4-NO ₂ , 2-CF ₃	25.39	40.91	29.30	46.89	34.56
35c	3-CF ₃ -Ph	SO ₂	4-NO ₂ , 2-CF ₃	18.14	32.01	16.77	38.66	24.77
35d	2-CF ₃ -Ph	SO ₂	4-NO ₂ , 2-CF ₃	28.33	46.09	20.46	38.58	31.86
35f	3,4-F-Ph	SO ₂	4-NO ₂ , 2-CF ₃	33.58	48.09	19.47	37.26	32.90
35g	2,4-F-Ph	SO ₂	4-NO ₂ , 2-CF ₃	30.24	46.58	17.92	57.96	34.78
35h	4-OCF ₃ -Ph	SO ₂	4-NO ₂ , 2-CF ₃	100	100	100	100	100
35i	3-OCF ₃ -Ph	SO ₂	4-NO ₂ , 2-CF ₃	17.96	27.72	12.23	20.27	18.74
35l	2-OCF ₃ -Ph	SO ₂	4-NO ₂ , 2-CF ₃	28.79	38.97	17.77	51.74	31.87
35o	4-CF ₃ -2-Pyridine	SO ₂	4-NO ₂ , 2-CF ₃	100	100	100	100	100
35p	5-CF ₃ -2-Pyridine	SO ₂	4-NO ₂ , 2-CF ₃	46.46	57.66	45.03	58.47	51.54
42b (R)	4-CF ₃ -Ph	S	4-CN, 3-CF ₃	9.75	17.18	14.45	9.28	12.24
42c (R)	3-CF ₃ -Ph	S	4-CN, 3-CF ₃	13.14	19.45	14.31	8.91	13.43
42d (R)	2-CF ₃ -Ph	S	4-CN, 3-CF ₃	5.30	7.69	7.90	2.95	5.55
42g (R)	2,4-F-Ph	S	4-CN, 3-CF ₃	17.15	28.46	25.19	18.29	21.78
42h (R)	4-OCF ₃ -Ph	S	4-CN, 3-CF ₃	28.81	29.78	19.83	17.39	23.32
43a (R)	4-F-Ph	S	4-CN, 2-CF ₃	NA				
45b (R)	4-CF ₃ -Ph	SO ₂	4-CN, 3-CF ₃	20.19	26.76	17.47	31.42	23.34
45c (R)	3-CF ₃ -Ph	SO ₂	4-CN, 3-CF ₃	25.66	45.19	13.17	39.92	27.95
45d (R)	2-CF ₃ -Ph	SO ₂	4-CN, 3-CF ₃	34.75	44.31	32.23	37.30	36.89
45g (R)	2,4-F-Ph	SO ₂	4-CN, 3-CF ₃	42.25	60.20	42.26	60.90	50.58
45h (R)	4-OCF ₃ -Ph	SO ₂	4-CN, 3-CF ₃	18.82	31.56	18.91	31.195	24.33
46a (R)	4-F-Ph	SO ₂	4-CN, 2-CF ₃	100	100	85.55	100	96.17
52	2-CF ₃ -Ph	S	4-NO ₂ , 3-CF ₃	1.28	2.40	0.72	2.78	1.57

Table 2

Antiproliferative activity for enzalutamide derivatives. All data are mean values from triplicate experiments.



Compound	R ₁	R ₂	IC ₅₀ (μM)				
			22Rv1	DU-145	LNCaP	VCaP	Geo.mean
61b	4-CN, 3-CF ₃	4-CF ₃	63.58	100	9.37	30.06	36.58
62b	4-NO ₂ , 3-CF ₃	4-CF ₃	100	100	2.12	73.13	35.28
62c	4-NO ₂ , 3-CF ₃	3-CF ₃	100	100	15.16	100	62.40
63b	4-CN, 2-CF ₃	4-CF ₃	100	100	8.36	100	53.78
63c	4-CN, 2-CF ₃	3-CF ₃	59.31	100	18.3	100	57.40
64b	4-NO ₂ , 2-CF ₃	4-CF ₃	16.39	100	3.73	100	27.96
64c	4-NO ₂ , 2-CF ₃	3-CF ₃	5.01	7.88	4.07	13.26	6.80
65b	3-CF ₃	4-CF ₃	100	100	5.95	72.40	45.56
65c	3-CF ₃	3-CF ₃	60.68	100	5.61	75.66	40.05
71b	4-CF ₃	3-CF ₃	92.47	100	16.59	100	57.34
71d	2-CF ₃	3-CF ₃	100	100	28.28	100	77.79
5 (Enzal.)	—	—	31.76	32.27	11.47	53.04	28.10

standard (*S*)-enobosarm (**44e**), improving its activity up to 4-fold (i.e. **28m**, **28l**, **27c**, etc.). Modifications on aromatic ring A do not appear to significantly affect antiproliferative activity.

Structural modifications on the B ring profoundly influence the antiproliferative effect, improving or totally abolishing activity. In

particular, replacement of the original fluorine in the *para* position with a more lipophilic and bulkier trifluoromethyl moiety is associated with an improvement of anti-proliferative activity of an average of two fold (i.e. **3** vs **32b**; **45a** vs **45b**; **25a** vs **25b**; **34a** vs **34b**; **35a** vs **35b**). Introduction of the trifluoromethoxy group in the

para position does not have a significant effect or slightly decreases the activity if compared with $-\text{CF}_3$ analogues. The 4-CN group present in (*S*)-enobosarm (**44e**) slightly improves or leaves unaltered the antiproliferative activity, depending on the X linker and the substituent in the A ring (**44e**, **28e**, **29e**). Repositioning of the trifluoromethyl group from the *para* to the *meta* and the *ortho* position greatly improves antiproliferative activity up to ten-fold. The best results were obtained with a substituent in position *ortho*, either a CF_3 (**23d**) or an OCF_3 (**25l**) group. The IC_{50} values for each new derivative appear to be a combination of the substituent in the *meta* or *ortho* position of aromatic ring B, the linker (thioether analogues are the most active) and the substituent in the A ring (nitro derivatives perform slightly better than cyano analogues). Generally, all *meta* and *ortho* substitutions on the B ring performed better than standard bicalutamide, leading to a significant activity improvement. Replacement of the phenyl ring B with either a 4-trifluoromethyl pyridine or a 5-trifluoromethyl pyridine abolishes activity with only few exceptions (**25o**, **25p**), which are probably a consequence of the presence of a 4- NO_2 -2- CF_3 aromatic substituent in the A ring. Introduction of a second fluoro substituent in the B ring, such as a 2,4-fluoro, 2,3-fluoro, 4-CN,3-F or 4-CN,2- CF_3 , is in general associated with a better activity profile if compared with standard bicalutamide and enobosarm. In particular, the introduction of an extra trifluoromethyl group in the *ortho* position of enobosarm aromatic ring B improved its antiproliferative activity up to 4-fold (**28m** and **29m** vs **44e**).

No substantial differences were found between racemic and chiral (*R*)-bicalutamide derivatives (**22d** vs **42d**; **22c** vs **42c**), confirming that the observed superior efficacy of the *R*-bicalutamide is mainly due to metabolic properties [13].

Interestingly, the best-performing new compound was **52**, in which the central methyl group is replaced with a trifluoromethyl function. The IC_{50} (geometric mean of the overall antiproliferative activity in the four cell lines) is 3.5-fold better than its methyl analogue (**23d**), and the improvement is evident if compared with bicalutamide (50-fold).

Considering antiproliferative activity for each individual cell line, most of our compounds showed interesting results in all four cell types, with the best results found for those cells expressing the androgen receptor, such as LNCaP (the most sensitive cell line to the new derivatives). This evidence suggests that the newly synthesised structures retain an antagonistic effect on the androgen receptor. Significant antiproliferative activity was also found in the DU-145 cell line (the least sensitive to our new molecules), which does not express the androgen receptor and is insensitive to androgen activity, suggesting that also a different antiproliferative mechanism could be involved, along with the canonical anti-androgen receptor action. This potential off-target effect seems to be present also in the parent bicalutamide (**3**, **45a**), which shows similar IC_{50} values across the four cell lines, and might have been enhanced by the newly introduced modifications.

Newly synthesized enzalutamide analogues showed reduced activity in the antiproliferative assay in comparison with standard enzalutamide, with the only exception being **64c**. However, the new modifications clearly influenced the activity on LNCaP cells, improving enzalutamide IC_{50} up to five-fold (**62b**). The total absence of activity in the DU-145 cell line could be an indication of a pure anti-androgenic effect for these new compounds. Replacement of the original enzalutamide substituents in aromatic ring A with a *para* trifluoromethyl group is the most effective modification, while modifications on the B ring do not appear to significantly affect activity.

As a general consideration on the antiproliferative results, the introduction/change of position of trifluoromethyl and trifluoromethoxy groups emerges as an interesting strategy to

improve the biological effects of the parent molecules.

2.3. Androgen receptor (AR) agonist/antagonist assay

Twenty-two derivatives were selected for the evaluation of their AR antagonist/agonist effect using the GeneBLAzer[®] Betalactamase reporter technology for Nuclear receptors (NRs), to assess whether the antiproliferative activity found is related to any interference with the AR function [23].

All tested compounds were found to be antagonist of the androgen receptor in a single concentration antagonism experiment (10 μM concentration, antagonistic effect > 80%), which measures their ability to reduce the receptor activation induced by the known androgen receptor agonist R1881 [24,25]. A 10-concentration antagonism assay (Supplementary data) showed that the new molecules possess an antagonistic IC_{50} in the same range of reference (*R*)-bicalutamide and enzalutamide (Table 3). The (*R*)-bicalutamide IC_{50} is comparable with previously reported values in similar assays [26,27].

In the bicalutamide-derived series of analogues, the antagonistic effect is not influenced by the substituents in aromatic ring A (**28d** vs **23d** vs **25d** vs **22d**), with a small beneficial effect found for both the O and S linkers (**28d** vs **23d** vs **33d**) in the racemic derivatives, whereas the SO_2 linker is the most effective found for the (*R*) structures (**42b** vs **45b** and **45h**). Structural modifications on aromatic ring B have a major influence for antagonistic activity; substitutions in the *meta* position are associated with improved IC_{50} values (i.e. **28d**, **28l**, **23d**), substitutions in the *ortho* position are well tolerated (i.e. **23c**), while substitutions in the *para* position result in higher IC_{50} values (i.e. **42b**) if compared with (*R*)-bicalutamide. Overall, the results obtained fall in a similar range, with no significant changes in the anti-androgenic activity in comparison with control bicalutamide. The presence of a cyano group in the *para* position of ring B (**28m**, **28n**), as in control (*S*)-enobosarm, is associated with the best antagonistic activity, while the

Table 3

AR antagonist/agonist assay results. * Compounds were considered full antagonist if at a single concentration of 10 μM the reduction of receptor activation by R1881 was greater than 80%; ** Compound at 10 μM concentration in absence of R1881 was used; *** Compounds tested at 10 different concentrations; **** Due to poor solubility, the highest concentration used was 1 μM ; N.E., no antagonistic effect.

Compound	Antagonistic effect (%) [*]	Agonistic effect (%) ^{**}	IC_{50} (μM) ^{***}
45a (R-Bic.)	83	5	0.490
44e (S-Enob.)	59	26	0.0364
5 (Enzal.)	95	N.E.	0.361
22d	93	11	0.425
23c	93	N.E.	0.625
23d	91	4	0.280
25d	94	2	0.332
28d	94	7	0.183
28h	96	–	0.625
28i	106	–	0.407
28l	103	N.E.	0.198
28m	108	N.E.	0.0722
28n	65 ^{****}	N.E.	0.0492
29m	99	–	0.736
33d	85	1	0.811
33c	104	–	1.07
42b	92	9	2.170
45b	93	–	0.775
45h	61 ^{****}	N.E.	0.777
52	110	–	0.245
62b	91	–	0.0803
63b	96	–	0.402
64b	102	–	0.265
64c	87	–	0.111
65c	100	–	0.123

introduction of a second substituent is tolerated. Compound **52**, the best performing in the antiproliferative assay, showed an antagonistic IC_{50} comparable to the one of (*R*)-bicalutamide. Considering the enzalutamide series, no significant change in the antagonistic effect was observed for the new derivatives tested.

For 14 compounds, a further analysis was performed in order to verify any potential agonistic effect on the androgen receptor. The compounds were tested at a single concentration (10 μ M) under the same experimental conditions used for the antagonistic assay, in the absence of R1881. All new derivatives showed either total absence or an agonistic effect <10% (not significant), confirming their full antagonistic behaviour. The partial agonist nature of (*S*)-enobosarm (**44e**) was also confirmed in our assay: after an initial antagonistic activity at low concentration (best antagonistic IC_{50}), it acts as an agonist, activating the androgen receptor (agonistic effect >20%). Interestingly, the new ether analogues, which could be considered as enobosarm derivatives, were found to be full AR antagonists (i.e. **28m**, **28n**, **25d**, **28l**).

The AR antagonist/agonist assay confirmed a pure AR antagonistic nature for the newly prepared compounds, which showed a concentration-dependent antagonistic activity. Moreover, an activity switch from partial agonist to full antagonist can be observed for our enobosarm analogues.

No correlation between AR assay and antiproliferative data can be identified, implying that other modes of action or other parameters could play an important role in the antiproliferative activity found for our new compounds.

2.4. Molecular modelling studies

Due to the retained activity of the newly synthesised compounds on the AR, and in an attempt to investigate the switch from partial agonist to full antagonist found for the newly prepared enobosarm derivatives, a series of molecular modelling analyses was designed and carried out.

2.4.1. AR antagonist conformation homology model

The functional switch from the open (antagonist) to the closed (agonist) conformation of the AR is caused by the movement of helix 12 (AR-H12), one of the 12 helices that define the ligand-binding domain (LBD) [28,29]. The crystal structure of the complex bicalutamide-AR is only available in the closed conformation due to the W741L mutation (PDB ID: 1Z95), which causes bicalutamide to occupy the AR binding site in an agonist fashion, allowing the closure movement of helix 12 and therefore the activation of the AR [28,29]. For the purpose of this part of the study, a homology model of the human WT-AR open conformation was built, using a single template approach in the MOE2014 homology modelling tool following a previously reported methodology [30]. The crystal structure of the progesterone receptor in its open antagonistic form (PDB ID: 2OVM) was used as template, considering the good sequence identity (54%) with the human AR [31]. The final 3D model was obtained as the Cartesian average of 10 generated intermediate models [32]. Validation of the new model was performed using the Rampage Server, the Errat plot and calculating the RMSD with the 2AM9 crystal structure [33–35]. Fig. 3 shows the shift of helix 12 between the new model and the mutated AR-bicalutamide crystal (PDB ID: 1Z95) [28].

2.4.2. Docking studies

Docking of (*R*)-bicalutamide was performed in the LBD of the new model to evaluate its predicted antagonistic binding mode. As shown in Fig. 4, docked bicalutamide occupies the binding site in proximity of Trp741, forming a H-bond with Asn705 through its hydroxyl group, and most importantly interacting with Arg752

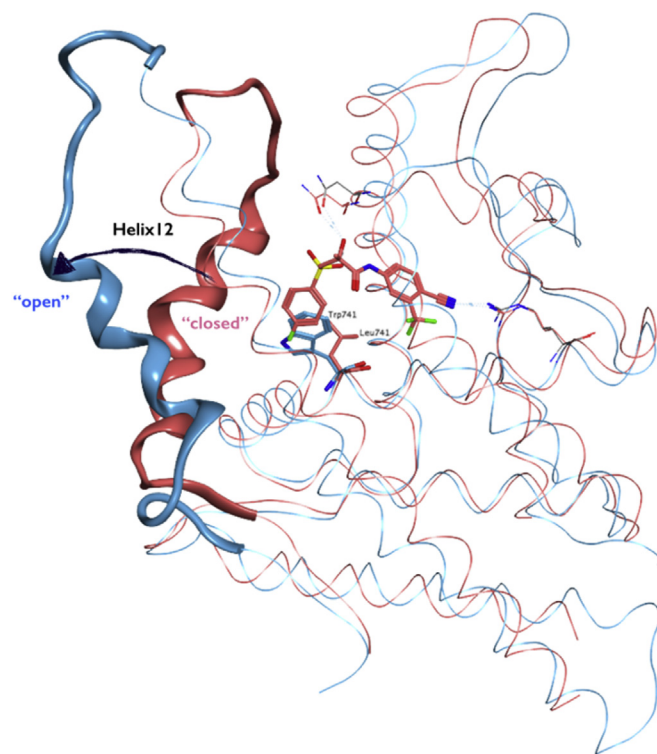


Fig. 3. Superposition between the crystal structure of the AR in the closed form (PDB ID: 1Z95) (pink) and the new open AR model (light blue). Mutated Leu741 (pink) reduces the steric hindrance in comparison with the non-mutated Trp741 (light blue). Co-crystallised bicalutamide (carbon atoms in salmon) is shown as stick model. (For interpretation of the references to colour in this figure legend, the reader is referred to the web version of this article.)

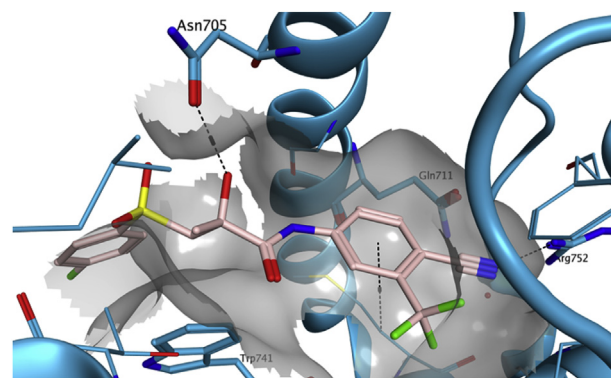


Fig. 4. Docking of (*R*)-bicalutamide (carbon atoms in pink) in the AR homology model (light blue). Bicalutamide occupies the binding site in proximity of Trp741. The occupational molecular surface around the active site is shown in grey. (For interpretation of the references to colour in this figure legend, the reader is referred to the web version of this article.)

through a second H-bond with its cyanide nitrogen [36]. A direct comparison with the bicalutamide-resistant AR crystal (Fig. 5) suggests that the sulfone ring orientation of the docking pose is the most plausible considering the presence of Trp741 and the position of helix 12. In fact, in the crystal, due to a W741L mutation, the sulfone aromatic ring is pointing down towards the centre of the protein, lying in the position that would be occupied by the Trp741 indole ring, allowing helix 12 closure [36]. The presence of Trp741 in the model does not allow this disposition (steric clash), orienting aromatic ring B toward helix 12, thus blocking its closure. Docking

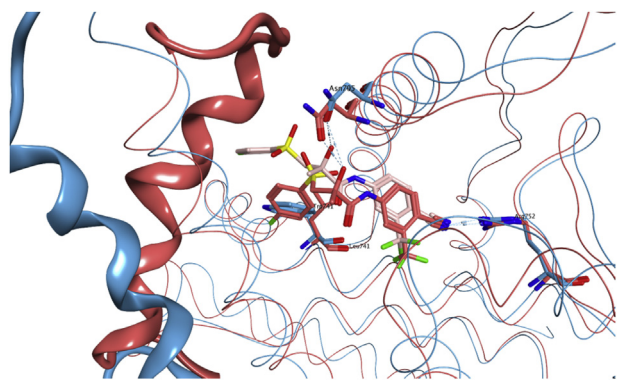


Fig. 5. Comparison between our AR model (light blue) and bicalutamide-resistant AR crystal 1Z95 (pink). Crystallised (carbon atoms in salmon) and docked bicalutamide (carbon atoms in pink) highlighted. (For interpretation of the references to colour in this figure legend, the reader is referred to the web version of this article.)

of the more rigid enzalutamide (Fig. 6) confirms the proposed antagonistic binding mode (comparable to the crystal structure of AR-LDB in complex with an enzalutamide-like compound, PDB ID: 3V49) [37].

Fig. 7 shows the docking of two newly designed compounds (**28m**, **33d**, **52**) in the AR homology model. The three compounds show a consistent binding mode, occupying the LBD in the same manner as bicalutamide, maintaining the same key interactions, consistently with the AR assay results.

Replacement of the fluorine substituent in the B ring with a bigger group such as trifluoromethyl or trifluoromethoxy, increasing the steric hindrance of this part of the molecule, could allow the overcoming of bicalutamide resistance mechanism. This speculation is supported by the docking of **33d** in the mutant AR crystal structure 1Z95: as shown in Fig. 8, the bulkier substituent in the B ring does not fit in the AR closed conformation, even in the presence of the adaptive mutation W741L, as indicated by the close proximity of ring B to the protein surface. Biological confirmation of this effect will be the focus of future studies.

Molecular docking of the new enobosarm derivatives (i.e. **28d**, **28m**, **28n**, **28i**, **25d**) was performed on the crystal structure of closed-conformation WT-AR in complex with (*S*)-enobosarm (PDB ID: 3RLJ) [38], in order to explain the observed activity switch from partial AR agonist to full antagonist. (*S*)-Enobosarm, after binding the AR and acting as antagonist, activates the receptor by favouring the closure movement of helix 12 even in the absence of the W741L mutation. This movement, as shown in the crystal structure, is

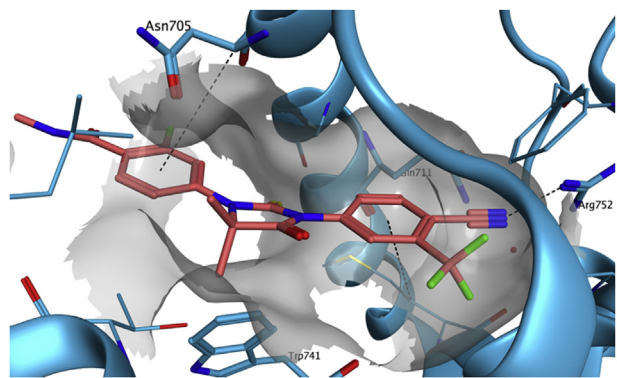


Fig. 6. Docking of enzalutamide (carbon atoms in salmon) in the AR homology model (light blue). The occupational molecular surface around the active site is shown in grey. (For interpretation of the references to colour in this figure legend, the reader is referred to the web version of this article.)

made possible by the more flexible and less bulky oxygen linker, which allows a binding conformation similar to the one found for bicalutamide in the W741L AR mutant crystal structure (Fig. 9). Docking results show that the replacement of the cyano substituent in aromatic ring B with a larger group (i.e. 2-OCF₃ in **28i** or 2-CF₃ in **28d**), or the introduction of a second aromatic substituent (i.e. 2-CF₃ in **28m**), might lead to structural clashes with helix-12, confirming that these new enobosarm derivatives could impede the movement of helix 12 to the AR-closed conformation, hence the absence of any residual AR agonistic activity (Fig. 10).

The results obtained for our new enobosarm analogues might represent a further indication that the newly inserted structural modifications could play a role in overcoming the problem of bicalutamide-induced AR mutation W741L.

2.4.3. Molecular dynamics simulations

To further confirm the reliability of the new homology model, and consequently support the speculations on the binding mode proposed for the newly synthesized compounds, 5 ns molecular dynamics (MD) simulations for selected derivatives (**45a**, **23d**, **25d**, **28d**, **33d**, **62b**), either free in solution or in complex with the AR, were performed. These structures were selected in order to cover the range of activities found in the AR antagonist assay. The MD output results were used to compute $\Delta G_{\text{binding}}$ energy calculations of the ligand-protein complexes (Table 4).

The stability showed by most of the ligand-protein systems during the simulations could be a consequence of the active site composition, mainly formed by hydrophobic amino acids (Met745, Met787, Leu707, Leu704, Leu712, Val746, Trp741, Phe764, etc.), which provides an ideal environment for the lipophilic nature of these fluorinated molecules. Moreover, the formation of two hydrogen bonds in the bicalutamide/enobosarm derivatives, both present during the entire MD duration, with Arg752 and Asn705, further contribute to the system stability, allowing the molecules to maintain a stable conformation in the active site. The lowest calculated $\Delta G_{\text{binding}}$ was obtained for **62b**, whereas **33d**, a derivative with one of the highest antagonistic IC₅₀ values, showed the highest energy result. Interestingly, a similar correlation between the calculated $\Delta G_{\text{binding}}$ energy and the AR antagonistic IC₅₀ was found for all the compounds studied. Enzalutamide derivative **62b** showed the best result in terms of $\Delta G_{\text{binding}}$, confirming the best antagonistic IC₅₀ value obtained from the assay and highlighting the high affinity of the rigid enzalutamide-like structure for the androgen receptor. The $\Delta G_{\text{binding}}$ /AR antagonistic IC₅₀ correlation might represent a further confirmation of the reliability of the new AR homology model and of the proposed binding mode for the new fluorinated compounds.

2.5. *In vitro* metabolic stability, cell permeability and cytotoxicity studies

The significant improvement obtained with the newly synthesized analogues in the antiproliferative assay, which is associated with retained AR antagonistic activity in comparison with the reference compounds, could be a consequence of an off-target effect, already present in the parent structures and enhanced by the new modifications, or a consequence of altered cellular metabolism, stability and/or cell permeability of the new molecules, due to their high fluorine content.

In order to address these two points, additional *in vitro* studies on a selection of our most active compounds (**22c**, **22d**, **23c**, **23d**, **27b**, **28m**, **33d**, **42b**, **42c**) were performed. Metabolic stability, cell permeability and general cytotoxicity were evaluated. (*R*)-Bicalutamide (**45a**) and (*S*)-enobosarm (**44e**) were used in control experiments.

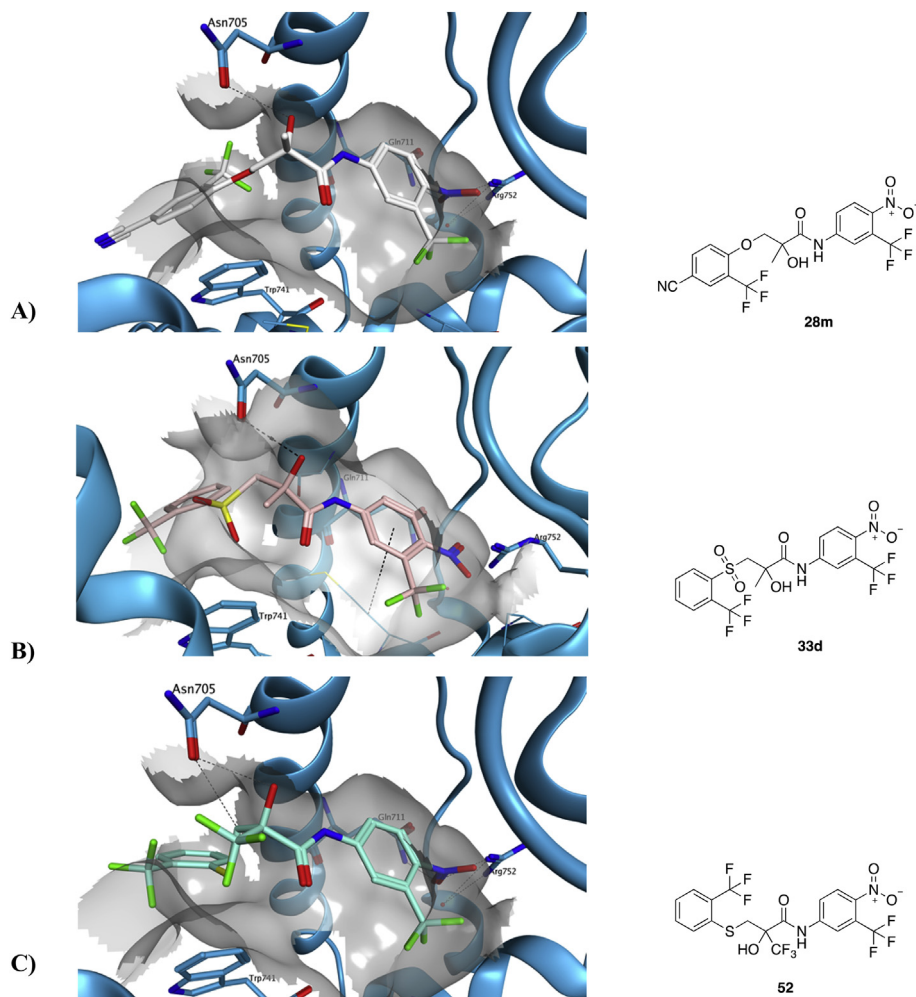


Fig. 7. Predicted binding mode of new derivatives **28m**, **33d** and **52** in the AR homology model.

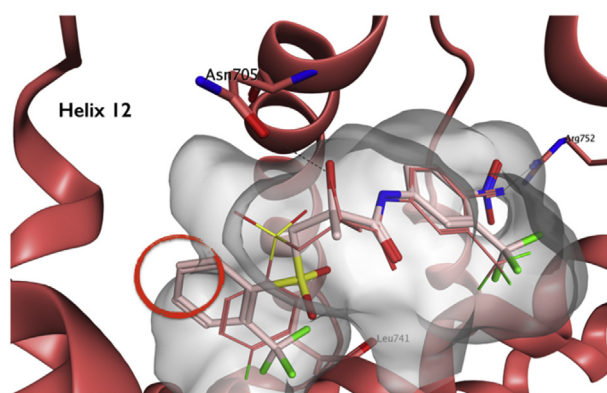


Fig. 8. Docking of **33d** (carbon atoms in light pink) in the 1295 crystal structure. The red circle highlights how the ring B of the new compound is in close proximity to the protein surface, potentially causing steric clashes that might impede the helix 12 movement to the closed conformation of the W741L AR mutant. The occupational molecular surface of the binding site is shown in grey. (For interpretation of the references to colour in this figure legend, the reader is referred to the web version of this article.)

2.5.1. Metabolic stability in liver microsomes

The selected compounds together with the controls were tested for their stability (oxidative metabolism being the predominant

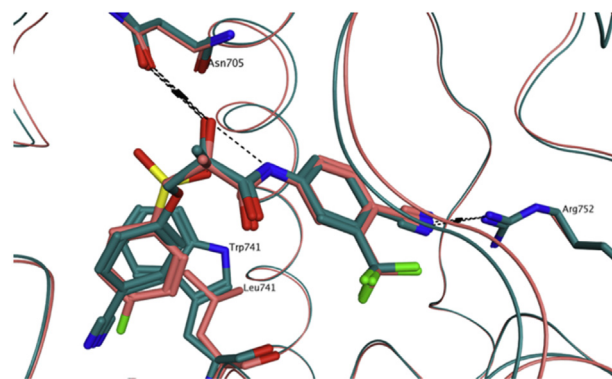


Fig. 9. Superimposition between the crystal structure of WT-AR co-crystallised with (*S*)-enobosarm (green) and the W741L-AR co-crystallized with bicalutamide (salmon). (For interpretation of the references to colour in this figure legend, the reader is referred to the web version of this article.)

type of biotransformation) in human liver microsomes (phase I drug metabolism). The tested compounds were incubated for 45 min with pooled liver microsomes (Supplementary data), and the intrinsic clearance (CL_{int}) and half-life ($t_{1/2}$) values were calculated based on 5 time points (Table 5). Bicalutamide, as reported in the literature, mainly undergoes oxidation in humans by

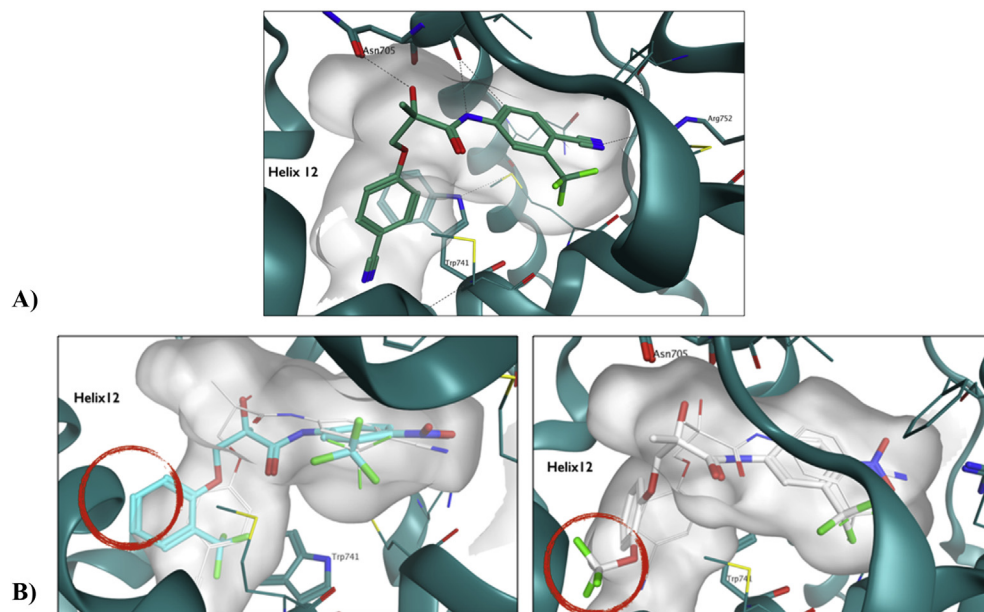


Fig. 10. A) (*S*)-Enobosarm co-crystallized in the WT-AR closed conformation (PDB ID: 3RLJ). B) Docking of **28d** (carbon atoms in turquoise) and **28l** (carbon atoms in white) in the 3RLJ crystal structure. Replacement of the cyano substituent with a bulkier group might cause structural clashes (red circles) with helix-12. (For interpretation of the references to colour in this figure legend, the reader is referred to the web version of this article.)

Table 4

Calculated ligand-interaction energies for the compounds analysed by Molecular Dynamics and antagonistic IC₅₀ values.

Compound	$\Delta G_{\text{binding}}$ (kJ/mol)	IC ₅₀ (μM)
62b	−13.425	0.0803
28d	−9.586	0.183
23d	−8.909	0.280
25d	−6.793	0.332
45a (R-bic.)	−2.521	0.490
33d	0.781	0.811

cytochrome P450 enzymes [26].

As expected, intrinsic clearance (Cl_{int}) is high and, as consequence, $t_{1/2}$ is very low for **22c**, **22d**, **23c**, **23d**, **42b**, **42c**. These compounds are thioethers and therefore they might undergo rapid oxidation of their sulfide linker to the corresponding sulfoxide and eventually to the sulfone. Ether derivatives **28m**, **27b** and (*S*)-enobosarm and sulfones **33d** and (*R*)-bicalutamide show lower Cl_{int} and higher $t_{1/2}$, with some of them showing complete metabolic stability (no loss of the parent detected during the assay). Oxidative metabolism seems to affect mainly the thioether linker with a small effect on the aromatic systems.

Interestingly, introduction of a trifluoromethyl group in the aromatic ring (**33d**) completely abolishes any oxidative metabolism on the ring itself, doubling the $t_{1/2}$ in comparison with (*R*)-bicalutamide. The significant antiproliferative activity found for thioether and ether derivatives does not seem to be caused by any oxidative metabolite, as indicated by the high stability of ether analogues and by the decrease in antiproliferative activity found for the respective sulfone derivatives. Moreover, these results suggest that ether derivatives have the best antiproliferative and stability (low intrinsic clearance) profile, making them good potential drug candidates.

2.5.2. Caco-2 cell permeability

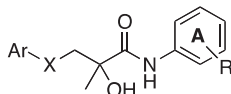
An *in vitro* Caco-2 bi-directional permeability assay was performed to gain information on membrane penetration, efflux from cells and possible interaction with the P-glycoprotein (P-gp) for the

new compounds. The data obtained are reported in Table 6 as apparent permeability (P_{app}) and efflux ratio. Generally, compounds with a P_{app} A \rightarrow B between 2 and $20 \times 10^{-6} \text{ cm s}^{-1}$ are considered as medium permeability drugs, whereas an efflux ratio (BA/AB) higher than 2 is an indication that the compound could be a substrate for a drug transporter (i.e. P-gp, BCRP) and undergo active efflux to the extracellular compartment. These transporters are all over-expressed in cancer cells and are commonly responsible for drug resistance [21,39].

(*R*)-Bicalutamide (**45a**) shows a P_{app} A \rightarrow B value of $32.0 \times 10^{-6} \text{ cm s}^{-1}$, which is comparable to the one reported in literature ($22.1 \times 10^{-6} \text{ cm s}^{-1}$), as both of these values would fall into the rank order category of good permeability [21]. Under the test conditions the P_{app} B \rightarrow A value was found to be $38.1 \times 10^{-6} \text{ cm s}^{-1}$, indicating membrane permeability in both directions for (*R*)-bicalutamide. The calculated efflux ratio (BA/AB) of 1.19 indicates that (*R*)-bicalutamide is not an efficient substrate for transporters, in discordance with published data, in which bicalutamide shows an efflux ratio (BA/AB) of 5.4 [21]. This discrepancy could be a consequence of using (*R*)-bicalutamide (**45a**), since bicalutamide enantiomers have different metabolism, permeability and absorption properties *in vivo*, which influence their biological activity [13] and possibly the interaction with the P-glycoprotein. Moreover, several experimental variables can influence the transport of compounds in both membrane directions. Due to this variability, the Caco-2 cell data have been used only to verify if any relevant difference in cell permeability is present among the tested compounds. The reliability of our assay and the functional presence of the protein transporters were evaluated using two standard reference compounds (atenolol for low permeability and propranolol for high permeability) and one known P-glycoprotein substrate (talinalol) (Supplementary data). The new molecules appear to be moderately permeable ($2 < P_{\text{app}}$ A \rightarrow B $< 20 \times 10^{-6} \text{ cm s}^{-1}$), with a low tendency to efflux from the cell. Differences between racemic and (*R*) derivatives are evident comparing compounds **22c** and **42c**, in which the pure (*R*) enantiomer has an increased efflux ratio, still lower than 2. Overall, the

Table 5

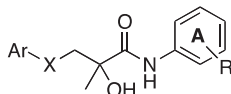
Metabolic stability in human liver microsomes; * CL_{int} : theoretical unrestricted maximum clearance of unbound drug by an eliminating organ, in absence of blood or plasma protein binding limitations; ** SE: standard error; ***Compounds metabolically stable with no loss of parent detected for the duration of the assay.



Compound	Ar (B ring)	X	R (A ring)	Metabolic stability		
				CL_{int} ($\mu\text{L}/\text{min}/\text{mg}$ protein)*	SE CL_{int} **	$t_{1/2}$ (min)
45a (R-Bic.)	4-F-Ph	SO ₂	4-CN, 3-CF ₃	6.48	2.52	214
44e (S-Eno)	4-CN-Ph	O	4-CN, 3-CF ₃	Metabolically Stable***		
22c	3-CF ₃ -Ph	S	4-CN, 3-CF ₃	232	5.89	5.97
22d	2-CF ₃ -Ph	S	4-CN, 3-CF ₃	379	12.8	3.66
23c	3-CF ₃ -Ph	S	4-NO ₂ , 3-CF ₃	202	2.33	6.87
23d	2-CF ₃ -Ph	S	4-NO ₂ , 3-CF ₃	409	46.8	3.39
27b	4-CF ₃ -Ph	O	4-CN, 3-CF ₃	Metabolically Stable***		
28m	4-CN,2-CF ₃ -Ph	O	4-NO ₂ , 3-CF ₃	2.59	2.45	534
33d	2-CF ₃ -Ph	SO ₂	4-NO ₂ , 3-CF ₃	Metabolically Stable***		
42b	4-CF ₃ -Ph	S	4-CN, 3-CF ₃	248	11.8	5.60
42c	3-CF ₃ -Ph	S	4-CN, 3-CF ₃	302	5.66	4.59

Table 6

Caco-2 cell permeability test; * (A → B): apical-basolateral flux; ** (B → A): basolateral-apical flux; this information was used for the apparent permeability (P_{app}) evaluation; ***Efflux Ratio: Mean P_{app} B → A/Mean P_{app} A → B; †Compounds tested under standard conditions using HBSS buffer at pH = 7.4. All other compounds were tested under the same conditions but the cell media contained BSA (1% w/v). All compounds were tested an initial concentration of 10 μM .



Compound	Ar (B ring)	X	R (A ring)	Permeability data		
				Mean P_{app} (A → B) ($\times 10^{-6}$ cm s ⁻¹)*	Mean P_{app} (B → A) ($\times 10^{-6}$ cm s ⁻¹)**	Efflux ratio BA/AB***
45a (R-Bic.) †	4-F-Ph	SO ₂	4-CN, 3-CF ₃	32.0	38.1	1.19
44e (S-Eno.) †	4-CN-Ph	O	4-CN, 3-CF ₃	31.5	26.7	0.848
22c	3-CF ₃ -Ph	S	4-CN, 3-CF ₃	3.92	4.73	1.21
22d	2-CF ₃ -Ph	S	4-CN, 3-CF ₃	3.08	7.12	2.31
23c	3-CF ₃ -Ph	S	4-NO ₂ , 3-CF ₃	5.00	4.27	0.853
23d	2-CF ₃ -Ph	S	4-NO ₂ , 3-CF ₃	3.44	2.90	0.843
27b	4-CF ₃ -Ph	O	4-CN, 3-CF ₃	5.09	4.80	0.943
28m	4-CN,2-CF ₃ -Ph	O	4-NO ₂ , 3-CF ₃	4.35	3.49	0.803
33d †	2-CF ₃ -Ph	SO ₂	4-NO ₂ , 3-CF ₃	13.3	17.2	1.29
42b	4-CF ₃ -Ph	S	4-CN, 3-CF ₃	5.80	4.74	0.817
42c	3-CF ₃ -Ph	S	4-CN, 3-CF ₃	6.84	12.2	1.78

results obtained suggest that these compounds do not show any significant difference in cell permeability in comparison with the standards, therefore no correlation can be identified between antiproliferative data and cell permeability properties.

2.5.3. Cell viability assay (MTT)

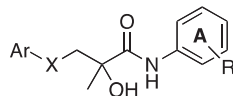
A MTT cell viability assay was performed in a human hepatocarcinoma (HepG2) cell line, in order to evaluate the cytotoxicity profile and to further explore the possible presence of an off-target effect for the new compounds. The MTT assay measures the effect of molecules on cell proliferation and other events that eventually lead to cell death [40].

Data are reported in Table 7 as minimum effective concentration (MEC) related to a vehicle control (DMSO) and AC₅₀. All tested

compounds showed a concentration-dependent decrease in formazan production across the range studied (example plots in the Supplementary data), indicating a decrease in cell viability associated with some growth inhibitory and toxic effects. Compared with control (R)-bicalutamide (**45a**), the new compounds are in general characterized by a higher cytotoxicity, with the lowest MEC and AC₅₀ values obtained for **23d**, which is also one of the most active compounds in the antiproliferative assay (antiproliferative data Table 7).

These results might represent an important indication that the newly prepared analogues, besides the canonical AR antagonist activity, possess an extra effect, which positively contributes to their antiproliferative action. Such effect seems to be particularly evident for **23d**, while other derivatives (e.g. **28m**, **42b**) do not

Table 7
MTT assay; all the compounds have been tested at 8 different concentrations. * MEC: minimum effective concentration that significantly crosses vehicle control threshold; ** AC50: concentration at which 50% of maximum effect is observed; ***Geometric mean.



Compound	Ar (B ring)	X	R (A ring)	MTT test		Antiproliferative data
				MEC (μM)*	AC ₅₀ (μM)**	Abs. IC ₅₀ (μM)***
45a (R-Bic.)	4-F-Ph	SO ₂	4-CN, 3-CF ₃	19.2	54.3	47.05
44e (S-Eno.)	4-CN-Ph	O	4-CN, 3-CF ₃	21.8	32.8	27.41
22c	3-CF ₃ -Ph	S	4-CN, 3-CF ₃	18.4	36.6	7.23
22d	2-CF ₃ -Ph	S	4-CN, 3-CF ₃	14.7	25.8	6.16
23c	3-CF ₃ -Ph	S	4-NO ₂ , 3-CF ₃	13.2	26.1	7.04
23d	2-CF ₃ -Ph	S	4-NO ₂ , 3-CF ₃	1.71	2.73	5.17
27b	4-CF ₃ -Ph	O	4-CN, 3-CF ₃	11.3	23.9	9.15
28m	4-CN,2-CF ₃ -Ph	O	4-NO ₂ , 3-CF ₃	10.6	20.2	6.71
33d	2-CF ₃ -Ph	SO ₂	4-NO ₂ , 3-CF ₃	22.7	32.6	26.50
42b	4-CF ₃ -Ph	S	4-CN, 3-CF ₃	49.6	61.2	12.24
42c	3-CF ₃ -Ph	S	4-CN, 3-CF ₃	26.6	34.6	13.43

show a significant increase in cytotoxicity, maintaining instead a remarkable improvement in the antiproliferative assay in comparison with bicalutamide. The mechanism and effect (necrosis, apoptosis, reduction of cellular proliferation or effect on mitochondria) causing this cytotoxicity, which seems to be a consequence of the new structural modifications, will be the main focus of future studies.

3. Conclusions

The structures of bicalutamide and enzalutamide, two non-steroidal androgen receptor antagonists in use to treat prostate cancer, have been chemically modified leading to the synthesis of new and more potent antiproliferative compounds. Different chemical modifications have been planned in order to benefit from the properties of fluorine in improving the activity and pharmacological profile of drugs. The novel chemical entities were found to be full androgen receptor (AR) antagonists, with no residual agonist effect found also for structural analogues of enobosarm (ether derivatives), a well-known AR partial agonist. Introduction of extra perfluoro groups (CF₃ and OCF₃) confers metabolic stability to phase I drug metabolizing enzymes, maintaining the same good membrane permeability of the parent compounds. A very notable improvement in the *in vitro* anti-proliferative effect on four different PC cell lines (VCap, LNCaP, DU-145 and 22RV1) has been achieved, improving the activity of the parent structures up to 50 folds, thus making some of the new molecules potential drug candidates for the treatment of prostate cancer. This marked activity improvement did not parallel an enhanced AR antagonistic effect. Moreover, increased cytotoxicity found for some of the new analogues in the MTT assay could be an indication that the compounds developed in this work, while certainly binding to AR LBD and exhibiting full antagonist behaviour, might possess another biological effect, which positively contributes to their anti-proliferative action in the prostatic cancer cell lines. The reliable AR homology model prepared and all the docking information provided can offer useful insights for the development of pure AR antagonists. The new model appears well validated by all observed data.

The results achieved in this work will be the starting point for further modification of the parent compounds, in order to improve both antiproliferative and anti-androgen properties. All successful structural modifications will be further investigated, giving priority

to the replacement of the central methyl group of bicalutamide with a CF₃ (**52**).

Future biological studies will aim to understand the mechanism of action and the biological consequences of potential off target effects, along with the evaluation of our novel AR antagonists in a W741L mutant AR. Finally, the most promising compound for each structural family (**23d**, **27b**, **33d**) has been selected for *in vivo* pre-clinical studies in mouse models.

4. Experimental

All chemistry, biology and molecular modelling experimental procedures, along with compound characterisation, are fully described in the Supplementary Data. All final compounds were purified by column chromatography or recrystallization, fully characterised by NMR (¹H, ¹³C, ¹⁹F) and LRMS. HRMS is reported for representative final compounds (one example for each synthetic method). All final compounds were found to be >95% pure by HPLC.

Acknowledgments

The authors would like to thank Oncotest (Freiburg, Germany) for provision of human prostate cancer cell line testing as an outsourced service. The AR binding assays were carried out by Invitrogen (location), and Cyprotex (U.K.) were responsible for performing the metabolic stability, cell permeability and HepG2 cytotoxicity assays as an outsourced service. Mr Derek Angus is warmly acknowledged for many valuable comments on the ADME section of the manuscript. The Welsh Government is acknowledged for funding (A4B-Academic Expertise for Business grant), in collaboration with Catylix, Inc (Burbank, CA, USA) as industrial advisers to the project.

Appendix A. Supplementary data

Supplementary data related to this article can be found at <http://dx.doi.org/10.1016/j.ejmech.2016.04.052>.

References

- [1] J. Ferlay, H.-R. Shin, F. Bray, D. Forman, C. Mathers, D.M. Parkin, Estimates of worldwide burden of cancer in 2008: GLOBOCAN 2008, *Int. J. Cancer* 127 (2010) 2893–2917.
- [2] G.J.C.M. Kolvenbag, P. Iversen, D.W.W. Newling, *Antiandrogen monotherapy:*

- a new form of treatment for patients with prostate cancer, *Urology* 58 (2001) 16–22.
- [3] H.I. Scher, W.K. Kelly, Flutamide withdrawal syndrome: its impact on clinical trials in hormone-refractory prostate cancer, *J. Clin. Oncol.* 11 (1993) 1566–1572.
- [4] P. Reid, P. Kantoff, W. Oh, Antiandrogens in prostate cancer, *Investig. New Drugs* 17 (1999) 271–284.
- [5] J. Anderson, The role of antiandrogen monotherapy in the treatment of prostate cancer, *BJU Int.* 91 (2003) 455–461.
- [6] M.P. Wirth, O.W. Hakenberg, M. Froehner, Antiandrogens in the treatment of prostate cancer, *Eur. Urol.* 51 (2007) 306–313.
- [7] D. O'Hagan, D.B. Harper, Fluorine-containing natural products, *J. Fluor. Chem.* 100 (1999) 127–133.
- [8] B.E. Smart, Fluorine substituent effects on bioactivity, *J. Fluor. Chem.* 109 (2001) 3–11.
- [9] J. Wang, M. Sánchez-Roselló, J.L. Aceña, C. del Pozo, A.E. Sorochinsky, S. Fustero, V.A. Soloshonok, H. Liu, Fluorine in pharmaceutical industry: fluorine-containing drugs introduced to the market in the last decade 2001–2011, *Chem. Rev.* 114 (2014) 2432–2506.
- [10] K.D. James, N.N. Ekwuribe, A two-step synthesis of the anti-cancer drug (*R,S*)-Bicalutamide, *Synthesis* 7 (2002) 850–852.
- [11] B.-C. Chen, R. Zhao, S. Gove, B. Wang, J.E. Sundeen, M.E. Salvati, J.C. Barrish, Nucleophilic aromatic substitution of methacrylamide anion and its application to the synthesis of the anticancer drug bicalutamide, *J. Org. Chem.* 26 (2003) 10181–10182.
- [12] Pizzatti, E.; Vigano, E.; Lussana, M.; Landonio, E. Procedure for the synthesis of bicalutamide. U.S. Patent 0,041,161, February 23, 2006.
- [13] I.D. Cockshott, Bicalutamide: clinical pharmacokinetics and metabolism, *Clin. Pharmacokinet.* 13 (2004) 855–878.
- [14] Dalton, T.J.; Miller, D.D.; Yin, D.; He, Y. Selective androgen receptor modulators and methods of use thereof. U.S. Patent 6,569,896 B2 May 27, 2003.
- [15] H. Tucker, G.J. Chesterson, Resolution of the nonsteroidal antiandrogen 4'-cyano-3'-[(4-fluorophenyl)sulfonyl]-2-hydroxy-2-methyl-3'-(tri-fluoromethyl)-propionanilide and the determination of the absolute configuration of the active enantiomer, *J. Med. Chem.* 31 (1988) 885–887.
- [16] Y. He, D. Yin, M. Perera, L. Kirkovsky, N. Stourman, W. Li, J.T. Dalton, D.D. Miller, Novel nonsteroidal ligands with binding affinity and potent functional activity for the androgen receptor, *Eur. J. Med. Chem.* 37 (2002) 619–634.
- [17] M.E. Jung, S. Ouk, D. Yoo, C.L. Sawyers, C. Chen, C. Tran, J. Wongvipat, Structure-activity relationship for thiohydantoin androgen receptor antagonist for castration-resistant prostate cancer (CRPC), *J. Med. Chem.* 7 (2010) 2779–2796.
- [18] H. Yoshino, H. Sato, T. Shiraishi, K. Tachibana, T. Emura, A. Honma, N. Ishikura, T. Tsunenari, M. Watanabe, A. Nishimoto, R. Nakamura, T. Nakagawa, M. Ohta, N. Takata, K. Furumoto, K. Kimure, H. Kawate, Design and synthesis of an androgen receptor pure antagonist (CH5137291) for the treatment of castration-resistant prostate cancer, *Biorg. Med. Chem.* 18 (2010) 8150–8157.
- [19] Jain, R.P.; Angelaud, R.; Thompson, A.; Lamberson, C.; Greenfield, S. Process for the synthesis of diarylthiohydantoin and diarylhydantoin compounds. WO Patent 0,657,0 A1 September 1, 2011.
- [20] D.J. Hwang, J. Yang, H. Xu, I.M. Rakov, M.L. Mohler, J.T. Dalton, D.D. Miller, Arylthiohydantoin selective androgen receptor modulators (SARMs) for prostate cancer, *Biorg. Med. Chem.* 14 (2006) 6525–6538.
- [21] A. Colabufo, V. Pagliarulo, F. Berardi, M. Contino, C. Inglese, M. Niso, P. Ancona, G. Albo, A. Pagliarulo, R. Perrone, Bicalutamide failure in prostate cancer treatment: involvement of multi drug resistance proteins, *Eur. J. Pharmacol.* 601 (2008) 38–42.
- [22] H. Kuruma, H. Matsumoto, M. Shiota, J. Bishop, F. Lamoureux, C. Thomas, D. Briere, G. Los, M. Gleave, A. Fanjui, A. Zoubeidi, A novel antiandrogen, compound 30, suppresses castration-resistant and MDV3100-resistant prostate cancer growth *in vitro* and *in vivo*, *Mol. Cancer. Ther.* 12 (2013) 567–576.
- [23] Receptor Assays section. <http://www.lifetechologies.com/uk> (accessed July 1, 2015).
- [24] W.R. Kelce, E. Monosson, M.P. Gamcsik, S.C. Laws, L.E. Gray Jr., Environmental hormone disruptors: evidence that vinclozolin developmental toxicity is mediated by antiandrogenic metabolites, *Toxicol. Appl. Pharmacol.* 126 (1994) 276–285.
- [25] C.L. Waller, B.W. Juma, L.E. Gray Jr., W.R. Kelce, Three-dimensional quantitative structure-activity relationships for androgen receptor ligands, *Toxicol. Appl. Pharmacol.* 137 (1996) 219–227.
- [26] W. Gao, J. Kim, J.T. Dalton, Pharmacokinetics and pharmacodynamics of nonsteroidal androgen receptor ligand, *Pharm. Res.* 8 (2006) 1641–1658.
- [27] T.A. Thompson, G. Wilding, Androgen antagonist activity by the antioxidant moiety of vitamin E, 2,2,5,7,8-pentamethyl-6-chromanol in human prostate carcinoma cells, *Mol. Cancer. Ther.* 2 (2003) 797–803.
- [28] C.E. Bohl, W. Gao, D.D. Miller, C.E. Bell, J.T. Dalton, Structural basis for antagonism and resistance of bicalutamide in prostate cancer, *Proc. Natl. Acad. Sci. U. S. A.* 102 (2005) 6201–6206.
- [29] C. Helsen, T. Van de Broeck, A. Voet, S. Prekovic, H. Van Poppel, S. Joniau, F. Claessens, Androgen receptor antagonists for prostate cancer therapy, *Endocr. Relat. Cancer* 4 (2014) T105–T118.
- [30] M.S. Gomaa, A. Brancale, C. Simons, Homology model of 1 α ,25-dihydroxyvitamin D₃ 24-hydroxylase cytochrome P450 24A1(CYP24A1): active site architecture and ligand binding, *J. Steroid Biochem. Mol. Biol.* 104 (2007) 53–60.
- [31] K.P. Madauss, E.T. Grygielko, S.J. Deng, A.C. Sulpizio, T.B. Stanley, C. Wu, S.A. Short, S.K. Thompson, E.L. Stewart, N.J. Laping, S.P. Williams, J.D. Bray, A structural and *in vitro* characterization of asoprisnil: a selective progesterone receptor modulator, *Mol. Endocrinol.* 21 (2007) 1066–1081.
- [32] K. Pereira de Jesus-Tran, P.-L. Cote, L. Cantin, J. Blanchet, F. Labrie, R. Breton, Comparison of crystal structures of human androgen receptor ligand-binding domain complexed with various agonists reveals molecular determinants responsible for binding affinity, *Protein Sci.* 15 (2006) 987–999.
- [33] Rampage, <http://mordred.bioc.cam.ac.uk/~rapper/rampage.php> (accessed Aug 20, 2015).
- [34] C. Colovos, T.O. Yeates, Verification of protein structures: patterns of nonbonded atomic interactions, *Protein Sci.* 2 (1993) 1511–1519.
- [35] Molecular Operating Environment, http://www.chemcomp.com/MOEMolecular_Operating_Environment.htm. (accessed Aug 20, 2014).
- [36] N. Lallous, K. Dalal, A. Cherkasov, P.S. Rennie, Targeting alternative sites on the androgen receptor to treat castration-resistant prostate cancer, *Int. J. Mol. Sci.* 14 (2013) 12496–12519.
- [37] F. Nique, S. Hebbe, C. Peixoto, D. Annot, J.-M. Lefrancois, E. Duval, L. Michoux, N. Triballeau, J.M. Lemoullec, P. Mollat, M. Thauvin, T. Prange, D. Minet, P. Clement-Lacroix, C. Robin-Jagerschmidt, D. Fleury, D. Guedin, P. Deprez, Discovery of diarylhydantoins as new selective androgen receptor modulators, *J. Med. Chem.* 55 (2012) 8225–8235.
- [38] C.B. Duke, A. Jones, C.E. Bohl, J.T. Dalton, D.D. Miller, Unexpected binding orientation of bulky-B-ring anti-androgens and implications for future drug targets, *J. Med. Chem.* 54 (2011) 3973–3976.
- [39] J.W. Polli, S.A. Wring, J.E. Humphreys, L. Huang, J.B. Morgan, L.O. Webster, C.S. Serabjit-Singh, Rational use of *in vitro* P-glycoprotein assays in drug discovery, *J. Pharmacol. Exp. Ther.* 299 (2001) 620–628.
- [40] P. Senthilraja, K. Kathiresan, *In vitro* cytotoxicity MTT assay in Vero, HepG2 and MCF-7 cell lines study of marine yeast, *J. Appl. Pharm. Sci.* 03 (2015) 080–084.